A&A manuscript no.
(will be inserted by hand later)

Your thesaurus codes are:
03(12.07.1; 11.04.1; 09.04.1; 03.13.4)

ASTRONOMY AND ASTROPHYSICS
October 13, 1998

Redshift estimate of a gravitational lens from the observed reddening of a multiply imaged quasar

C. Jean and J. Surdej*

Institut d'Astrophysique, Université de Liège,
Avenue de Cointe 5, B-4000 Liège, Belgium

Received / Accepted

Abstract. Light rays from a multiply imaged quasar usually sample different path lengths across the deflector. Extinction in the lensing galaxy may thus lead to a differential obscuration and reddening between the observed macro-lensed QSO images. These effects naturally depend on the precise shape of the extinction law and on the redshift of the lens. By means of numerical Monte-Carlo simulations, using a least-squares fitting method and assuming an extinction law similar to that observed in the Galaxy, we show how accurate photometric observations of multiply imaged quasars obtained in several spectral bands could lead to the estimate of the lens redshift, irrespective of the visibility of the deflector. Observational requirements necessary to apply this method to real cases are thoroughly discussed. If extinction laws turn out to be too different from galaxy to galaxy, we find out that more promising observations should consist in getting high signal-to-noise low resolution spectra of at least three distinct images of a lensed quasar, over a spectral range as wide as possible, from which it should be straightforward to extract the precise shape of the redshifted extinction law. Very high signal-to-noise, low spectral resolution, VLT observations of H1413+117 and MG 0414+0534 should enable one to derive such a redshifted extinction law.

Key words: gravitational lensing – Galaxies: redshifts – dust, extinction – Methods: numerical

1. Introduction

For the case of several known gravitational lens systems, the deflector is either not yet detected or it is so faint that its redshift remains unknown (see the Gravitational Lensing web page at `http://vela.astro.ulg.ac.be/grav_lens/`). Measurement of the deflector redshift is mandatory in order to properly model the corresponding gravitational lens systems. Usually, the lens redshift is determined from spectroscopic observations of either emission lines due to the lensing galaxy or of galaxy absorption lines detected in the spectra of the QSO images. In this work, we present an alternate method to derive the redshift of a too faint and/or an invisible lens. First, we describe the method which is based upon the fitting of photometric observations with a redshifted extinction model and we then show results from Monte Carlo simulations. The latter turn out to be very useful in order to assess the errors affecting the estimate of the lens redshift. Next, we attempt to apply this method to several known gravitational lens systems and outline all observational requirements needed in order to derive successful results. Finally, we propose a generalization of this method. Conclusions form the last section.

Send offprint requests to: C. Jean, jean@astro.ulg.ac.be
* Directeur de Recherches du FNRS (Belgium)

2. Description of the method

2.1. Generalities

Figure 1 depicts a gravitational lens system. The light rays emitted from the quasar are deflected by the lensing galaxy and the resulting macro images are reddened because of extinction effects in the deflector. Due to the different path lengths across the galaxy, differential reddening results between the macro lensed components.

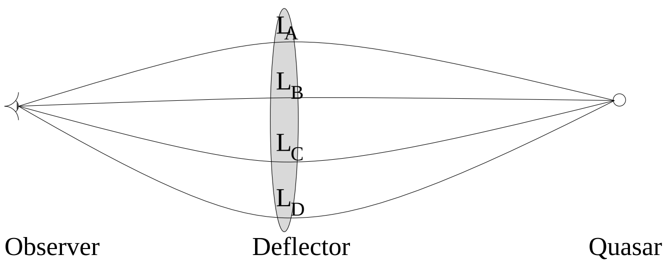

Fig. 1. Schematic representation of a multiply imaged quasar. $L_A - L_D$ denote different path lengths across the deflector.

The flux received by the observer from component i at a wavelength λ is:

$$F^i_\lambda = F^0_\lambda A_i e^{-\mathrm{Ext}(\lambda', R_V) L_i} \quad (1)$$

where F_λ^0 is the flux that would be observed from the quasar in the absence of lensing, A_i the macro lens amplification of component i, $\mathrm{Ext}(\lambda', R_V)$ the Galaxy dust opacity at the wavelength $\lambda' = \frac{\lambda}{1+z_l}$ (z_l being the lens redshift) and $R_V = \frac{A(V)}{E(B-V)}$ (see Cardelli *et al.* 1989), and L_i the path length of component i through the deflector.

When deriving Eq. (1), we have of course implicitly assumed that the macro lensed images are not contaminated by light from the lensing galaxy, that they are not affected by microlensing effects, that no intrinsic colour variations exist between the lensed components, that the law of extinction (first assumed to be alike that of the Galaxy) is similar all through the deflector and that the observed reddening takes place in a single lensing plane. A check on the applicability of most of these conditions can be made as suggested in section 2.3.

The colour of component i, between the wavelengths λ_1 and λ_2, is then merely given by:

$$m_{\lambda_1,i} - m_{\lambda_2,i} = -2.5 \log \left(\frac{F^0_{\lambda_1}\, e^{-\mathrm{Ext}(\lambda'_1, R_V) L_i}}{F^0_{\lambda_2}\, e^{-\mathrm{Ext}(\lambda'_2, R_V) L_i}} \right). \quad (2)$$

Having chosen one of the macro-lensed images as a reference component (i.e. $i = \mathrm{ref}$), the relative colour of component j (i.e. $i = j$) may be expressed as:

$$(m_{\lambda_1,j} - m_{\lambda_2,j}) - (m_{\lambda_1,\mathrm{ref}} - m_{\lambda_2,\mathrm{ref}}) = \frac{2.5}{\ln(10)} \mathcal{L}_j \left[\mathrm{Ext}(\lambda'_1, R_V) - \mathrm{Ext}(\lambda'_2, R_V)\right] \quad (3)$$

where $\mathcal{L}_j = L_j - L_{\mathrm{ref}}$ represents the relative path length of component j.

2.2. Observational constraints from the measurement of colours

If we assume that the gravitational lens system consists of N macro lensed components and that observations are being carried out through M filters, we easily find that there are $M-1$ independent colours for each of the $N-1$ components (the reference component is of course not included). Thus, there results a set of $(M-1)(N-1)$ equations alike Eq. (3).

Besides, there are 2 unknowns which do not depend on the numbers of filters and components: z_l and R_V. Moreover, for each of the $N-1$ components, there is one additional unknown: $\mathcal{L}_i$. Consequently, we have a total of $2 + (N-1) \times 1 = N+1$ unknowns.

Since we must have more equations than unknowns, we easily establish the necessary condition:

$$(M-1)(N-1) \geqslant N+1 \quad \text{i.e.} \quad M(N-1) \geqslant 2N. \quad (4)$$

For $N = 2$, 3, or 4, we easily find out that $M \geqslant 4$, 3 or $\frac{8}{3}$, i.e. a minimum of 4, 3 or 3 filters is requested, respectively. Therefore, observational data of multiply imaged quasars acquired through several photometric filters are mandatory.

Note that if data obtained in M filters come from several different observing runs, it is then safer to only use those colours formed between filters from the same run and hence we finally get less than $M-1$ useful colours. The above necessary condition may consequently not be any longer fulfilled.

2.3. Colour-colour diagrams

Before applying the proposed method, we must make sure that in a colour-colour diagram, and in accordance with Eq. (3), the measurements of the various lensed components are approximately located along a straight line. Otherwise, it may mean that one or more of the conditions listed in section 2.1 are not fulfilled.

Secondly, the differential reddening for most of the components has to be significantly larger than the observational errors. Otherwise, the slope of the straight line in the colour-colour diagram remains too uncertain. For example, the components of the gravitational lens systems PG 1115+080 (Kristian *et al.* 1993) and B 1422+231 (Yee & Ellingson 1994; Yee & Bechtold 1996) have very similar colours and hence these cases are not appropriate for application of this method. Promising candidates are H1413+117 (see an example of colour-colour diagram in Fig. 2) and especially MG 0414+0534 which is known to be very stable (Moore & Hewitt 1997) and probably not affected by significant microlensing effects (McLeod *et al.* 1998).

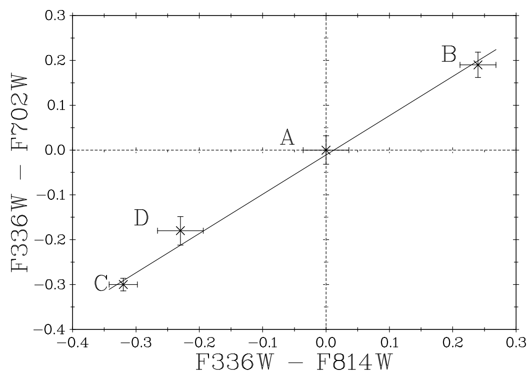

Fig. 2. Example of a colour-colour diagram for the case of H1413+117, constructed from observational data listed in Table 2. Image A has been selected as the reference component.

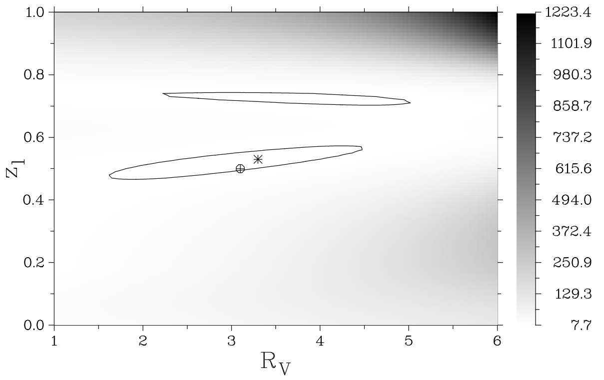

Fig. 3. χ^2 map from simulations of '5 filters' observations, adopting $R_V = 3.1$, $z_l = 0.5$, $\mathcal{L} = 0, 0.6, 1.3, 1.1$ for components A, B, C and D, respectively and a noise of 0.1 mag. for the simulated U, B, V, R and I magnitudes. The symbols $\oplus$ and $*$ correspond to the input and calculated values of the z_l and R_V parameters.

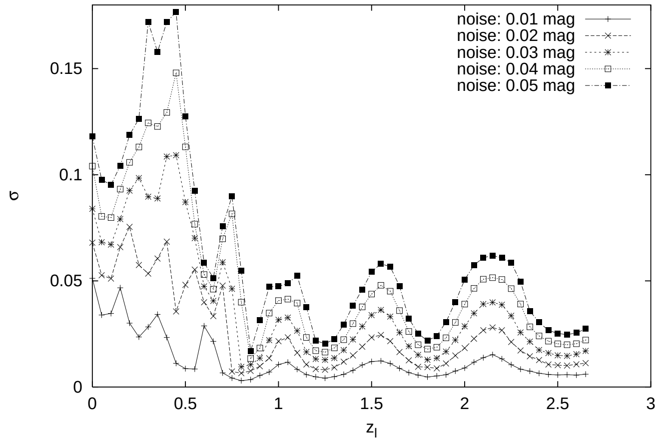

Fig. 4. Lens redshift dispersion σ versus the lens redshift z_l for five different levels of noise and adopting $R_V = 3.1$, $\mathcal{L} = 0, 0.6, 1.3, 1.1$ for components A, B, C and D, respectively. The photometric observations have been simulated for the five U, B, V, R and I Johnson filters.

2.4. *Fitting of the measured colours*

The left side of equation (3), which corresponds to an experimental relative colour, is directly derived from photometric observations of the macro lensed quasar images.

The right side of equation (3), and more explicitly the quantity "$\mathrm{Ext}(\lambda_1', R_V) - \mathrm{Ext}(\lambda_2', R_V)$", is systematically computed for different contiguous values of R_V and z_l using the Galaxy extinction law from Cardelli *et al.* (1989). The relative path lengths $\mathcal{L}_i$ are fitted using a routine that minimizes the following χ^2:

$$\chi^2 = \sum \frac{(\text{Experimental colour} - \text{Fitted colour})^2}{\sigma^2_{\text{Experimental colour}}}. \quad (5)$$

Figure 3 presents such a χ^2 map obtained from a set of simulated data (see below).

3. Simulations

In order to study the errors affecting the estimate of the lens redshift using the fitting method described above, we have carried out a wide range of Monte Carlo simulations. When doing these, we first fix the values of the following parameters: the lens redshift z_l within a defined interval, the parameter R_V usually set to 3.1 - corresponding to the average galactic value -, the relative macro-amplification $\mathcal{A}_i = \frac{A_i}{A_{\text{ref}}}$ and the relative path length $\mathcal{L}_i$ through the deflector for each lensed component so that we can calculate precise relative magnitudes for as many different filters as we wish. Then we add to these magnitudes a Gaussian noise of a certain level and apply the above fitting method. We repeat these two last steps 100 times and calculate the dispersion σ in the estimate of the lens redshift and the R_V parameter.

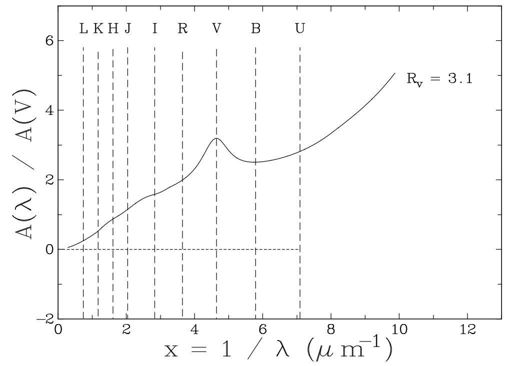

Fig. 5. Extinction law of Cardelli *et al.* for $R_V = 3.1$. The redshifted ($z = 1.55$) positions of selected filters are indicated.

Carrying out such simulations for different contiguous values of the theoretical lens redshift and for levels of noise comprised between 0.01 mag. and 0.05 mag., we obtain the curves illustrated in Fig. 4 for which we used the set of the five U, B, V, R and I Johnson filters. We see that the dispersion σ affecting the estimate of z_l is about 0.1 and even less at higher redshifts. The visible "oscillations" in Fig. 4 correspond to the positions of the wavelengths of the different selected filters with respect to the redshifted 2175 Å absorption bump (see Cardelli *et al.* 1989). As an example, Fig. 5 represents the extinction law of Cardelli *et al.* (1989) as a function of the reciprocal wavelength $\frac{1}{\lambda}$ for $R_V = 3.1$. The redshifted ($z = 1.55$) positions of the U, B, V, R, I, J, H, K and L filters are indicated.

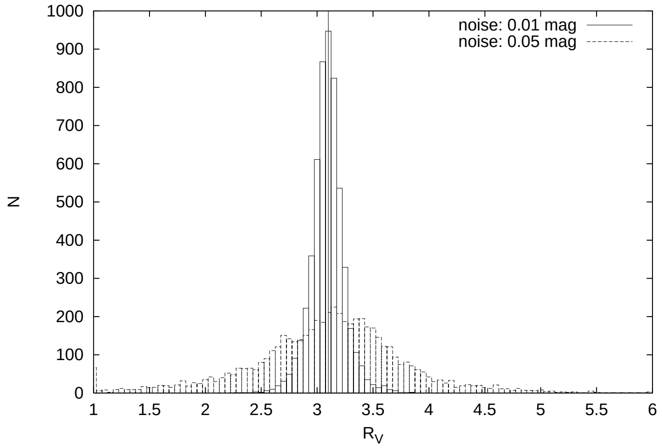

Fig. 6. Histograms of the repartition of R_V for two different levels of noise and adopting $R_V = 3.1$, z_l from 0 to 2.65 and $\mathcal{L} = 0, 0.6, 1.3, 1.1$ for components A, B, C and D, respectively (see Fig. 4).

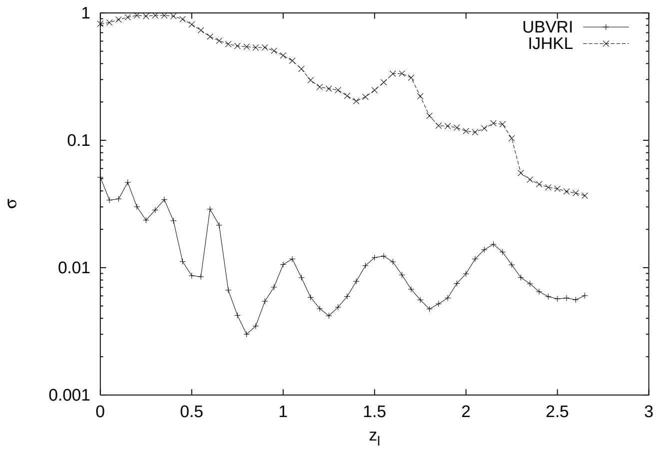

Fig. 7. Lens redshift dispersion σ versus the lens redshift z_l for two different sets of filters and adopting $R_V = 3.1$, $\mathcal{L} = 0, 0.6, 1.3, 1.1$ for components A, B, C and D, respectively. A noise of 0.01 mag. has been used for the simulated photometric observations.

Furthermore, we have illustrated in Fig. 6 dispersions affecting the derived values of R_V for the cases of 5 filters and two different levels of noise: 0.01 mag. and 0.05 mag. We see that, in this latter case, the dispersion gets rather large.

Next, Fig. 7 shows on a logarithmic scale differences in the lens redshift dispersion when using the U, B, V, R and I filters or the infrared I, J, H, K and L filters. Since the method is sensitive to the extinction gradient between two filter wavelengths, the much higher dispersion derived for the infrared filters is mainly accounted for by the shallower shape of the extinction law in the infrared range. Moreover, the lower extinction in the infrared range also affects the dispersion in the estimate of the lens redshift because the experimental relative colours are smaller and hence the effects of noise get more pronounced.

Finally, we have also used other extinction laws such those proposed by Pei (Pei 1992) for the Milky Way ("MW"), the Large Magellanic Cloud ("LMC") and the Small Magellanic Cloud ("SMC"). From the same set of simulated data as in Fig. 3, Fig. 8 shows the resulting χ^2 curves. Comparable minima and lens redshift solutions are usually found for the MW and LMC laws. However, high quality photometric observations are mandatory in order to efficiently select the most likely lens redshift among acceptable solutions for the different extinction laws. Note that because of the noise in the simulated photometric data, the minimum for the MW curve in Fig. 8 is found at $z_l = 0.48$, instead of the theoretical value $z_l = 0.5$.

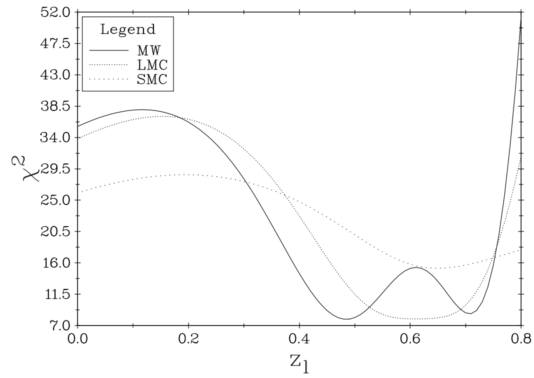

Fig. 8. χ^2 curves from simulations of '5 filters' observations adopting three different extinction laws and $R_V = 3.1$, $z_l = 0.5$, $\mathcal{L} = 0, 0.6, 1.3, 1.1$ for components A, B, C and D, respectively and a noise of 0.1 mag. for the simulated magnitudes (see text and Fig. 3).

4. Applications to some real gravitational lenses

4.1. 2237+0305

Figure 9 represents the χ^2 map for the Einstein Cross derived from the published sets of photometric observations listed in Table 1. The minimum is found for $z_l \simeq 0.13$. However, the redshift of this gravitational lens is known to be 0.04 (Huchra *et al.* 1985). The small discrepancy between these two redshift values is very likely due to the fact that the data were obtained during two different runs when photometric quality was not good enough ($\sigma \geqslant 0.02$ mag. for approximately half the reported values in Table 1). Moreover, this gravitational lens system is very likely affected by microlensing effects on a time scale of several years (Irwin *et al.* 1989; Corrigan *et al.* 1991; Østensen *et al.* 1996). The contours in Fig. 9 correspond to $\Delta\chi^2 = 1$ and delineate, at a confidence level of 68%, acceptable ranges for the values of z_l and R_V. Very high signal-to-noise photometric observations of the Einstein Cross, us-

Table 1. Photometry of 2237+0305

		Components				
Date	Filter	A	B	C	D	Reference[a]
25/09/87	g	17.77±0.03	17.98±0.03	18.46±0.05	18.69±0.06	1
25/09/87	r	17.62±0.02	17.77±0.03	18.06±0.04	18.40±0.06	1
25/09/87	i	17.25±0.02	17.38±0.02	17.61±0.03	17.98±0.04	1
10-11/10/95	B	17.626±0.009	17.741±0.008	18.881±0.020	19.111±0.033	2
10-11/10/95	V	17.278±0.004	17.428±0.009	18.389±0.009	18.734±0.022	2
10-11/10/95	R	17.093±0.004	17.274±0.004	18.109±0.008	18.441±0.010	2
10-11/10/95	I	16.966±0.006	17.192±0.007	17.910±0.015	18.206±0.020	2

[a](1) Yee 1988; (2) Burud et al. 1998 (CLEAN algorithm).

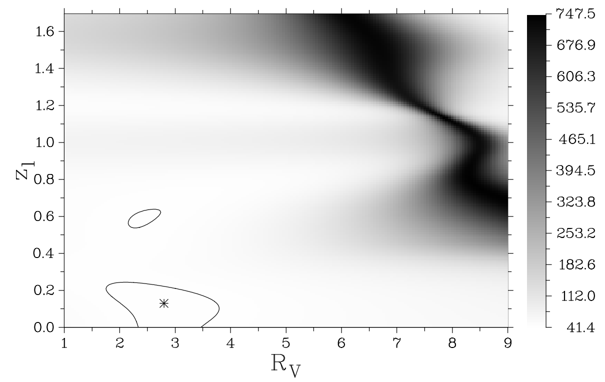

Fig. 9. χ^2 map for 2237+0305 derived from the published sets of photometric observations listed in Table 1. The χ^2 minimum corresponds to $z_l = 0.13$ and $R_V = 2.8$.

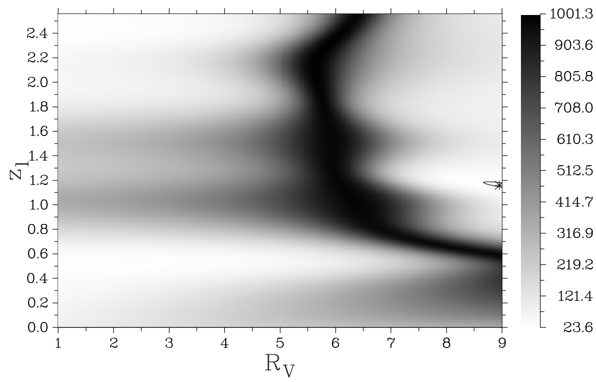

Fig. 10. χ^2 map for H1413+117 derived from the published sets of photometric observations listed in Table 2. The χ^2 minimum corresponds to $z_l = 1.15$ and $R_V \simeq 9$.

ing several filters during a single run and reliable tools to derive the photometry of the multiple QSO images, are badly needed to confirm that the different experimental relative colours reported between the lensed components are effectively, and solely, due to extinction effects in the deflector.

4.2. H1413+117

Figure 10 shows the χ^2 map for the Cloverleaf. For this case, we used photometric data obtained through 7 filters but from two distinct observing runs (see Table 2). We see that a minimum is found for $z_l \simeq 1.15$ and $R_V \simeq 9$. This latter value looks quite unexpected and we also conclude here that very high signal-to-noise photometric data of the Cloverleaf, using several filters during a single run, are badly needed to confirm that the reddening observed between the macro-lensed QSO images is essentially due to extinction effects. For this gravitational lens system, numerous lens redshifts from identified absorption lines have been proposed: 0.31 and 0.75 (Afanas'ev *et al.* 1996), 1.44 (Magain *et al.* 1988), 1.66, 1.87 and 2.07 (Hazard *et al.* 1984; Drew & Boksenberg 1984; Turnshek *et al.* 1988) but the real lens redshift still remains unknown.

4.3. MG 0414+0534

Figure 11 shows the χ^2 map for MG 0414+0534 derived from the published sets of photometric observations listed in Table 3. Because we only have 2 colours, including the near infrared colour H−K (see Table 3), the estimate of the lens redshift by this method remains very uncertain (see the very widespread contour in Fig. 11). Due to the known flux stability of MG 0414+0534 in the radio (Moore & Hewitt 1997), this gravitational lens system constitutes one of the most promising targets for an estimate of the lens redshift from the observed reddening of its lensed components. Microlensing effects must be insignificant for this object (McLeod *et al.* 1998). High quality and simultaneous photometric data from the visible up to the near infra-red are very much needed for this interesting system.

Table 2. Photometry of H1413+117

		Components				
Date	Filter	A	B	C	D	Reference[a]
02/08/94	B	-1.06±0.02	-0.82±0.02	-0.88±0.02	-0.70±0.02	1
02/08/94	V	-0.41±0.01	-0.23±0.01	-0.20±0.01	-0.06±0.01	1
02/08/94	R	-0.08±0.01	0.10±0.01	0.18±0.01	0.28±0.01	1
02/08/94	I	0.19±0.01	0.36±0.01	0.48±0.01	0.62±0.01	1
22/12/94	F336W	19.03±0.03	19.37±0.02	19.01±0.01	19.20±0.03	2
22/12/94	F702W	18.40±0.01	18.55±0.02	18.68±0.01	18.75±0.01	2
22/12/94	F814W	18.66±0.02	18.76±0.02	18.96±0.02	19.06±0.02	2

[a](1) Østensen et al. 1997; (2) Turnshek et al. 1997.

Table 3. Photometry of MG 0414+0534

		Components				
Date	Filter	A	B	C	D	Reference[a]
10/03/93	H	15.31±0.05	15.51±0.05	16.28±0.01	17.16±0.02	1
10/03/93	K	14.34±0.05	14.56±0.05	15.36±0.01	16.24±0.02	1
08/11/94	F675W	22.760±0.008	23.756±0.016	23.488±0.012	24.258±0.022	2
08/11/94	F814W	20.595±0.003	21.407±0.004	21.363±0.004	22.212±0.007	2

[a](1) McLeod et al. 1998; (2) Falco et al. 1997.

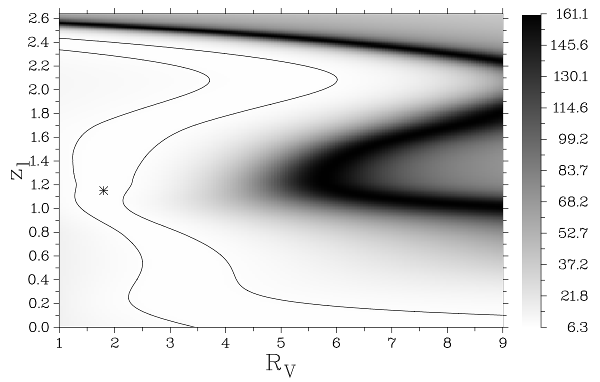

Fig. 11. χ^2 map for MG 0414+0534 derived from the published sets of photometric observations listed in Table 3. The χ^2 minimum corresponds to $z_l = 1.15$ and $R_V = 1.8$.

5. Generalization

From Eq. (1) and considering the j component relative to the *ref*(-erence) component, we may also write:

$$\frac{F_\lambda^j}{F_\lambda^{\rm ref}} = \frac{A_j}{A_{\rm ref}}\, e^{-{\rm Ext}(\lambda', R_V)[L_j - L_{\rm ref}]} = \mathcal{A}_j\, e^{-{\rm Ext}(\lambda', R_V)\mathcal{L}_j} \tag{6}$$

where $\mathcal{A}_j = \frac{A_j}{A_{\rm ref}}$. From this equation, we straightforwardly derive:

$$m_{\lambda,j} - m_{\lambda,{\rm ref}} = \frac{2.5}{\ln(10)}\, \mathcal{L}_j\, [{\rm Ext}(\lambda', R_V)] \; - 2.5\log(\mathcal{A}_j). \tag{7}$$

We see that in fact, one can also directly work with the relative magnitudes $m_{\lambda,j} - m_{\lambda,{\rm ref}}$ but that the relative macro lens amplifications $\mathcal{A}_j$ then appear as additional unknowns which also need to be fitted. Following a reasoning similar to that adopted in section 2.2, the necessary condition is also found to be: $M(N-1) \geqslant 2N$, where M and N have the same meaning. Before applying this generalized method to real photometric observations, one should make sure that intrinsic or extrinsic (cf. induced by micro-lensing) light variations are not affecting the individual lensed components. These conditions are of course more difficult to be checked than those imposed on the observed colours.

Finally, it is also straightforward to establish from Eq. (7) that the redshifted extinction law ${\rm Ext}(\lambda')$ may be directly retrieved as a function of λ' from the observed spectra of at least three multiple lensed QSO images. Very high signal-to-noise, low spectral resolution, VLT observations of gravitational lens systems like H1413+117 and MG 0414+0534 should enable one to derive such a redshifted extinction law and compare it with the known MW, LMC and SMC ones.

6. Conclusions

Monte Carlo simulations show that we need very accurate photometric data (typically $\sigma \simeq 0.01$ mag.), in several ($\gtrsim 4-5$) filters, in order to estimate the lens redshift from the differential reddening observed between the lensed images of a multiply imaged quasar. Furthermore, the macro-lensed images must not be affected by light contamination from the lensing galaxy, by microlensing effects or by intrinsic colour variations reflected with a time dependence between the lensed components. Unfortunately, all these conditions are rarely fulfilled at the same time and existing photometric data are often not good enough or not sufficiently reliable. Consequently, accurate photometric observations of gravitational lenses obtained in several filters during the same run are badly needed. Finally, we have seen that the redshifted extinction law of the lensing galaxy could be directly retrieved by means of a similar method provided that we may record the individual spectra of at least 3 lensed components, over a wide wavelength range, assuming that no light contamination, no microlensing effects, ... affect the individual lensed components. Very good such candidates to be observed with the VLT are H1413+117 and MG 0414+0534.

Acknowledgements. CJ is supported by contract ARC94/99-178 "Action de Recherche Concertée de la Communauté Française (Belgium)" and "Pôle d'Attraction Interuniversitaire, P4/05 (SSTC, Belgium)". JS would like to acknowledge support from the SSTC/PRODEX project "Observations of gravitational lenses".

Note added in proof: On the basis of spectroscopic observations obtained for MG 0414+0534 with the KECK telescope (see preprint astro-ph/9809063 submitted on 5 September 1998), J.L. Tonry and C.S. Kochanek report the redshift determination ($z_l \simeq 0.96$) of the very faint gravitational lens. Based upon preliminary photometric observations of this system, our own redshift estimate is found to be in reasonable agreement with this value (see Fig. 11).

References

Afanas'ev, V.L., Vlasyuk, V.V., Dodonov, S.N., Zhdanov, V.I., Mandzhos, A.V., Spiridonova, O.I. & Khmil', S.V., 1996, Kinematics and Physics of Celestial Bodies, Vol. 12, No. 5, pp. 7–11
Burud, I., Stabell, R., Magain, P., et al., 1998, available at `http://vela.astro.ulg.ac.be/preprint/index.html`
Cardelli, J.A., Clayton, G.C. & Mathis, J.S., 1989, ApJ, 345, 245
Corrigan, R.T., Irwin, M.J., Arnaud, J., et al., 1991, AJ, 102, 34
Drew, J.E. & Boksenberg, A., MNRAS, 1984, 211, 813
Falco, E.E., Lehár, J. & Shapiro, I.I., 1997, AJ, 113, 540
Hazard, C., Morton, D.C., Terlevich, R. & McMahon, R., 1984, ApJ, 282, 33
Huchra, J, Gorenstein, M., Kent, S., Shapiro, I., Smith, G., Horine, E. & Perley, R., 1985, AJ, 90, 691
Irwin, M.J., Webster, R.L., Hewett, P.C., Corrigan, R.T. & Jedrzejewski, R.I., 1989, AJ, 98, 1989
Kristian, J., et al., 1993, AJ, 106, 1330
Magain, P., Surdej, J., Swings, J.-P., et al., 1988, Nature, 334, 325
McLeod, B.A., Bernstein, G.M., Rieke, M.J. & Weedman, D.W., 1998, AJ, 115, 1377
Moore, C.B. & Hewitt, J.N., 1997, ApJ, 491, 451
Østensen, R., et al., 1996, A&A, 309, 59
Østensen, R., et al., 1997, A&AS, 126, 393
Pei, Y.C., 1992, ApJ, 395, 130
Turnshek, D.A., Foltz, C.B., Grillmair, C.J. & Weymann, R.J., 1988, ApJ, 325, 651
Turnshek, D.A., Lupie, O.L., Rao, S.M., et al., 1997, ApJ, 485, 100
Yee, H.K.C., 1988, AJ, 95, 1331
Yee, H.K.C. & Bechtold, J., 1996, AJ, 111, 1007
Yee, H.K.C. & Ellingson, E., 1994, AJ, 107, 28